# Qualitative failure analysis on laminate structures of windsurfing boards using analytical linear elastic modelling

N. Schwarzer, Technical University of Chemnitz, Institute of Physics, 09107 Chemnitz, Germany, Fax: ++493715313042, Tel: ++493715313210,
E-Mail: n.schwarzer@physik.tu-chemnitz.de
P. Heuer, ESAE, Am Lehmberg 11, 04838 Eilenburg, Germany, Fax: ++493423604159, Tel: ++491773844847, E-Mail: p.heuer@esae.de

## *Abstract*

Recently developed mathematical tools for the modelling of contact problems on thin film structures are adapted to allow the investigation of arbitrarily mixed purely isotropic and transversally isotropic laminate structures. The new tool is applied to model a variety of load problems resulting in the failure of windsurfing boards consisting of a relatively thin laminate shell and a soft polymer foam core. It is shown that local impact and distributed bending loads due to “bad landing” after high jumps or contact with parts of the sailing gear (the so called rig) especially the front part of the boom are leading to the most critical stress distributions resulting in failure. So most of the investigated boards were damaged because the rider (windsurfer) landed flat and thus produced a sudden impact force under his feet (impact defect). Other overloading occurred due to overturning of so called loop movements or the landing of the board exactly on respectively between two waves and this way producing high bending moments. Some of those typical loads are analysed in detail and the stresses occurring in the complex structure of the windsurfing boards are evaluated.
Keywords: Fibres, Foams, Layered Structures, Anisotropy, Fracture, Mechanical Properties, Analytical Modelling

## *Introduction*

Laminate structures are playing an important role everywhere it comes to combine lightness and flexibility with high stability and reliability. So numerous publications are available treating laminate composites with respect to the latter quality characteristics. Especially of interest has been the effect of impact and bending loads. So we find a lot of recently published papers treating the problem of contact and impact loading experimentally [1 - 6].

Especially interesting concerning the topic of this paper however is the work of Miyano et al [7] where laminate structures have been tested explicitly for the purpose of marine use. A crucial point is the determination of the mechanical properties of laminate structures. Here, indentation experiments have been proven of being of great use (see e.g. [8, 9]).
The determination of the mechanical properties by computational methods has been treated for example in [10 - 15]. While the latter papers have at least additionally applied analytical methods, there are many publication using only FE-Modelling in order to extract mechanical properties of laminate structures (e.g. [16 - 18]). The practically important problem of optimising laminate structures has been performed using failure signatures and safety criteria by Harik [19] and applying a so called Tabu search in [20].
In order to optimise windsurfing board laminate structures against impact and bending loads sufficiently fast evaluating approaches are required allowing to model contact problems on multi-layer structures for staked orthotropic, isotropic and transverse isotropic layers with a high number of relatively thin layers. Here, as we wanted to do "practical field studies directly on the spot" of application of laminated windsurfing boards, we needed a very fast evaluating relatively easy to use model. So, despite the fact that there are completely analytical models for the correct three dimensional description of mechanical contact problems on layered orthotropic materials available [21, 22], we needed to down scale these approaches in order to make them applicable for this project. Neglecting most of the unisotropic properties of the windsurfing board laminate structures we found, that in fact we obtained sufficiently good agreement with the observed failure mechanism by using a transversely isotropic approach (see part "Theory II" of this paper). The evaluation time was at least 100times faster than that of the approach presented in [21, 22]. The additional demand to make the model also usable and understandable for mathematically less trained team members (professional windsurfers for example) required a properly programmed surface [23].

A short survey especially considering the accuracy and the calculation time shall present the development of the approach used here. Applying the model of the layered half space and using the method of image loads or image contacts, Schwarzer has been able to model up to 4 layers including the substrate [24]. The approach brought very good agreement with experimental results in the case of single layer and bi-layer structures, but unfortunately it is not applicable on real multilayers with more than 5 layers. The main reason for this is due to the high calculation time increasing exponentially with the number of layers. The same holds for some other methods like the perturbation [25] or the boundary and the finite element

method [26]. There is a variety of publications about multilayered and graded coatings available [27 - 30], but non of them provides a sufficiently convenient and fast method allowing to treat contact problems on mixed pure and transversely isotropic or orthotropic laminate structures under contact loading as we want to consider here. It has been shown by Stone [31] (see also [32] and [33]), that in the case of a layered half space a sufficiently high number of layers can be modelled due to the method of integral transformation. He even modelled mixed pure and transversely isotropic layer structures under normal stress distribution. However in those cases, where the laminate structure is thin or in about the same scale as the area of the load applied on the laminated body in question, this method is not applicable due to numerical instabilities. So, if one for example wants to model impact and bending loads on hulls of boats, fuselages or other rather thin walled constructions the so called "model of the thick plate" is required. Thus, based on the approach of Lurie [34] Schwarzer [35] has developed a model allowing the investigation of thick layered plates under any arbitrary contact or bending load. The model has been included into a computer program evaluating mixed pure isotropic and transversely isotropic laminate structures with up to 100 different layers on an ordinary personal computer in an acceptable calculation time.

## *Theory I. – layered half space*

Apart from finite element or boundary element methods the integral transform method seems to be the only one allowing real multilayer modelling with more than 10 layers. As we are here only interested in contact areas of symmetry of revolution, we seek for a solution of the Navier equation for equilibrium in linear elasticity (see e.g. [31]) containing Bessel functions. Thus, the method is based upon the following approach for circular contact areas where, in the case of pure isotropy, the displacements within the i-th layer are given by:

$$\vec{u}_i = \begin{pmatrix} u_i \\ v_i \\ w_i \end{pmatrix} = c\int_0^\infty \begin{pmatrix} f(u)\left(\left(A+B+Buz\right)e^{uz} - \left(D-F+Fuz\right)e^{-uz}\right)J_1[ur]\dfrac{x}{r} \\ f(u)\left(\left(A+B+Buz\right)e^{uz} - \left(D-F+Fuz\right)e^{-uz}\right)J_1[ur]\dfrac{y}{r} \\ f(u)\left(\left(-A+\left(2-4\nu-uz\right)B\right)e^{uz} - \left(D+\left(2-4\nu+uz\right)F\right)e^{-uz}\right)J_0[ur] \end{pmatrix} du \qquad (1)$$

$J_n(z)$ denotes the Bessel function of the first kind of order n, x, y, z are the Cartesian co-ordinates with z being the axis of indentation and $r^2=x^2+y^2$. The function f(u) needs to be determined in accordance with the normal load distribution applied. So would for example a constant pressure distribution within a contact circle of radius a lead to (see e.g. [36]):

$$f(u)=\frac{a}{u}J_1[a\,u]\,. \tag{2}$$

The constant c must satisfy the condition, that the acting overall force F on the surface is opposite equal to the integral over the normal stress $\sigma_{zz}(r,\varphi,z)$ at this position (we set it z=0). Thus we have:

$$c=-\frac{F}{\int_0^{\infty}\int_0^{2\pi}\sigma_{zz}(r,\varphi,z=0)\,d\varphi\,dr}\,. \tag{3}$$

For transverse isotropic layers the approach must read:

$$\vec{u}_i=\begin{pmatrix}u_i\\ v_i\\ w_i\end{pmatrix}=c\int_0^{\infty}\begin{pmatrix} f(u)\left(Ae^{uz/\gamma_1}+Be^{uz/\gamma_2}-\left(De^{-uz/\gamma_1}+Fe^{-uz/\gamma_2}\right)\right)J_1[ur]\frac{x}{r}\\ f(u)\left(Ae^{uz/\gamma_1}+Be^{uz/\gamma_2}-\left(De^{-uz/\gamma_1}+Fe^{-uz/\gamma_2}\right)\right)J_1[ur]\frac{y}{r}\\ f(u)\left(m_1\left(\frac{A}{\gamma_1}e^{uz/\gamma_1}+\frac{D}{\gamma_1}e^{-uz/\gamma_1}\right)+m_2\left(\frac{B}{\gamma_2}e^{uz/\gamma_2}+\frac{F}{\gamma_2}e^{-uz/\gamma_2}\right)\right)J_0[ur]\end{pmatrix}du \tag{4}$$

The $\gamma_k$ (k=1, 2) have to be obtained from $\gamma_k^2=n_k$, whereas $n_k$ denote the two (real or conjugate complex) roots of the equation

$$A_{11}A_{44}n^2+\left[A_{13}\left(A_{13}+2A_{44}\right)-A_{11}A_{33}\right]n+A_{33}A_{44}=0\,. \tag{5}$$

The constants $m_k$ (k=1, 2) are related to $\gamma_k$ as

$$\frac{A_{11}\gamma_k^{\,2}-A_{44}}{A_{13}+A_{44}}=\frac{\left(A_{13}+A_{44}\right)\gamma_k^{\,2}}{A_{33}-\gamma_k^{\,2}A_{44}}=m_k \tag{6}$$

Rearranging all terms of (4) containing $\gamma_1$ and denoting the resulting function $F_1$ and doing the same with all term containing $\gamma_2$ obtaining a function $F_2$ the elastic field can be evaluated due to:

$$u+iv\equiv u^c=\Lambda\left(F_1+F_2+iF_3\right);\ \Lambda=\frac{\partial}{\partial x}+i\frac{\partial}{\partial y}\quad;\ w=m_1\frac{\partial F_1}{\partial z}+m_2\frac{\partial F_2}{\partial z}\,. \tag{7}$$

$$\sigma_1=2A_{66}\frac{\partial^2}{\partial z^2}\left(\left[\gamma_1^{\,2}-\left(1+m_1\right)\gamma_3^{\,2}\right]F_1+\left[\gamma_2^{\,2}-\left(1+m_2\right)\gamma_3^{\,2}\right]F_2\right), \tag{8}$$

$$\sigma_2=2A_{66}\Lambda^2\left(F_1+F_2\right), \tag{9}$$

$$\sigma_{zz} = A_{44}\frac{\partial^2}{\partial z^2}\left(\gamma_1^{\,2}\left(1+m_1\right)F_1+\gamma_2^{\,2}\left(1+m_2\right)F_2\right), \tag{10}$$

$$\tau_z = A_{44}\Lambda\frac{\partial}{\partial z}\left(\left(1+m_1\right)F_1+\left(1+m_2\right)F_2\right), \tag{11}$$

($\gamma_3^2=A_{44}/A_{66}$). To simplify the stress field the following combinations were used (Fabrikant [37]) $\sigma_1=\sigma_{xx}+\sigma_{yy}=\sigma_{rr}+\sigma_{\varphi\varphi}$, $\sigma_2=\sigma_{xx}-\sigma_{yy}+2i\tau_{xy}=e^{2i\varphi}\,(\sigma_{rr}-\sigma_{\varphi\varphi}+2i\tau_{r\varphi})$, $\tau_z=\tau_{xz}+i\tau_{yz}=e^{i\varphi}\,(\tau_{rz}+i\tau_{\varphi z})$ .

The yet unknown constants A,B, D and F have to be determined for each layer due to the boundary conditions at the interfaces of the multilayer structure. From equations (1) and (4) the complete elastic field at any point within the loaded laminate structure can be evaluated applying the formulae (8) to (11). For more information the reader is referred to the original works of Schwarzer [35], Fabrikant [37] and Stone [31]. A special software package has been developed in order to automate the calculations becoming immensely complex and cumbersome in the case of high numbers of layers [23, 38].

## *Theory II. – layered thick plate*

In order to obtain numerically stable approaches in the case of laminate structures being thin compared to the size of the contact zone (or in about the same scale), the integral transformation method must be substituted by a suitable series procedure. For our purpose here the following approaches will suffice:

Isotropic case i-th layer:

$$\vec{u}_i=\begin{pmatrix}u_i\\v_i\\w_i\end{pmatrix}=\sum_{n=1}^{\infty}c_n\begin{pmatrix}u^2\left(\left(A+B+Buz\right)e^{uz}-\left(D-F+Fuz\right)e^{-uz}\right)J_1\left[ur\right]\dfrac{x}{r}\\u^2\left(\left(A+B+Buz\right)e^{uz}-\left(D-F+Fuz\right)e^{-uz}\right)J_1\left[ur\right]\dfrac{y}{r}\\u^2\left(\left(-A+\left(2-4\nu-uz\right)B\right)e^{uz}-\left(D+\left(2-4\nu+uz\right)F\right)e^{-uz}\right)J_0\left[ur\right]\end{pmatrix} \tag{12}$$

transverse isotropic case i-th layer:

$$\vec{u}_i = \begin{pmatrix} u_i \\ v_i \\ w_i \end{pmatrix} = \sum_{n=1}^{\infty} c_n \begin{pmatrix} u^2\left(Ae^{uz/\gamma_1} + Be^{uz/\gamma_2} - \left(De^{-uz/\gamma_1} + Fe^{-uz/\gamma_2}\right)\right) J_1[ur]\dfrac{x}{r} \\ u^2\left(Ae^{uz/\gamma_1} + Be^{uz/\gamma_2} - \left(De^{-uz/\gamma_1} + Fe^{-uz/\gamma_2}\right)\right) J_1[ur]\dfrac{y}{r} \\ u^2\left(m_1\left(\dfrac{A}{\gamma_1}e^{uz/\gamma_1} + \dfrac{D}{\gamma_1}e^{-uz/\gamma_1}\right) + m_2\left(\dfrac{B}{\gamma_2}e^{uz/\gamma_2} + \dfrac{F}{\gamma_2}e^{-uz/\gamma_2}\right)\right) J_0[ur] \end{pmatrix} \quad (13)$$

The parameter u must now be set $u = \frac{\lambda_n}{r_0}$, with $\lambda_n$ denoting the n-th root of the equation $J_0(r)=0$. The parameter $r_0$ must be chosen such, that it is big compared to the lateral dimensions of the investigated laminate part and sufficiently small in order to reduce the number of terms of the series approach necessary to generate a proper surface load distribution. In the calculations presented here, up to 1000 terms were used.

## *Application to a variety of board failure problems in windsurfing*

### Windsurfing – some basics and the equipment

First sailing attempts with a prototype of a sailboard dates back to the late 1950's, when the founding father of windsurfing, Newman Darby, wanted to combine sailing and wave surfing. The first windsurf board was about 3.5m long and weighted 27kg and Darby was considered rather a weirdo than the man with a great vision he obviously was. Since then, many things have changed: as the material and shapes of the equipment developed constantly, heavy and unwieldy polyethylene boards were substituted by laminated board structures, the jumps and moves become more and more radical and windsurfing is nowadays one of the most popular water sports all over the world.

Windsurf equipment consists of two major parts: the complete rig with a mast making the rig stand upright, a sail to catch the wind, turn it into sail force and drive the craft, and a boom which spreads the sail and on which the windsurfer holds on, gives direction and controls the wind pressure and thus the speed.

The second part of the vehicle is the board (figures 1 and 2). The bow is very often called the board's nose and is bent slightly upwards. On the stern, also called tail, are three foot straps located, two front, and one hind strap (on some board, usually those for race or speed performances there could be also more straps), in which the rider (windsurfer) finds a foothold when sailing fast over rough (choppy) water and jumping. A certain area under those

foot straps is covered with rubber foot pads, making it more comfortable for the surfer, preventing him from slipping and finally protecting both rider and board against hard impact. A tail fin, or skag, is the main lateral pressure centre under water (lateral plane) when the board is planning (see below) and thus, sets up resistance against drifting off course.

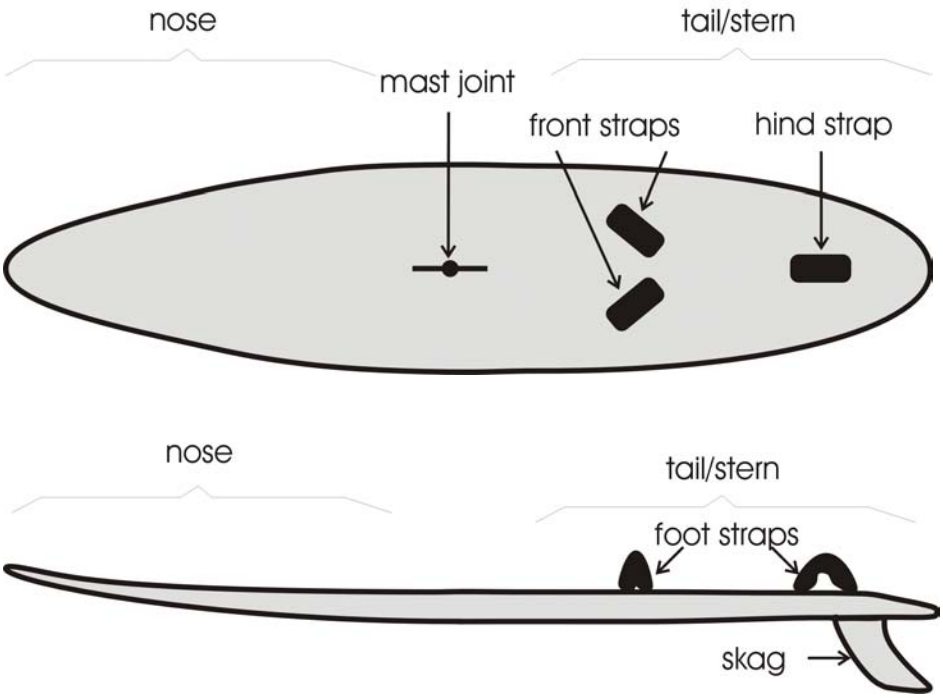


**Fig. 1 Main parts of a windsurfing board**

Depending on the purpose and shape, a modern typical wave board weights about 8 kg and has a length of 2.5m to 2.8m.

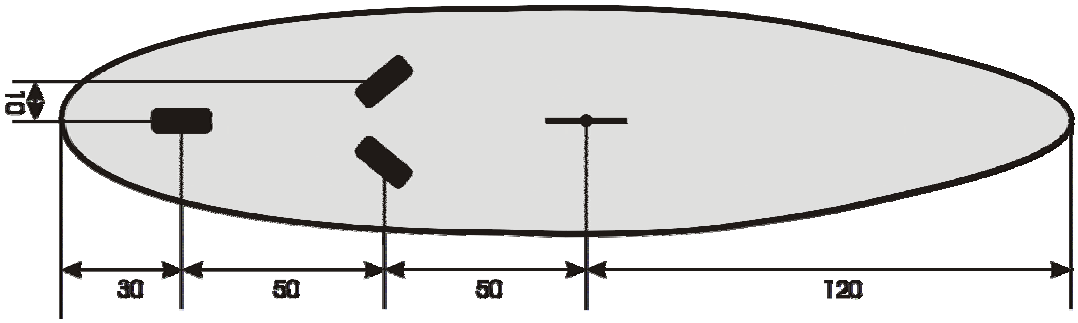


**Fig. 2 Co-ordinate system and measures of a typical wave board**

Both parts, rig and board, are connected by a flexible mast joint that allows the rig to be tilted in any direction. By tilting the rig and with that, changing the incidence angle toward the

wind, the sail force is moved whereas the lateral pressure centre (skag and all parts under water) stays the same and thus the board can be steered easily and without a rudder.
With a harness, which connects the rider's waist to the sail, the advanced windsurfer can transfer the power from the wind pressure caught in his sail to his body and with that, the required muscle power in hands and arms reduce to a bearable minimum so that even light and delicately built female windsurfers, even if very rare, could in principle practice this interesting sport without the need of special muscle training.
When the windsurfer gets faster, he is able to climb his own bow wave produced by his board when moving and thus, edging out water, and he will ride down this bow wave and becomes even faster. This state is called "planning" and now the rider can crawl into the foot straps and perform a great variety of so called speed moves and jumps (figures 3 and 4).

**Fig. 3 Number one reason for board failure: jumps**


**Fig. 4 "Willy Skipper": impact load on the nose part**

Some of the most popular and spectacular movements are so called loop jumps. Therefore, the rider jumps high into the air and turns his rig, his board and himself either forward or backward so that he lands -if all goes well- after one or even two full rotation in riding direction. But those moves together with almost all other forms of jumps are not only spectacular and create a stir, they are also dangerous for both: the windsurfer and the equipment.

## Board failure problems

A thorough analysis of the failure problems observable on windsurfing boards shows that there are two major mechanisms leading to damage. First, there are impact loads. They are mainly induced due to so called flat landing after high jumps (the rider lands his board flat on the water surface and thus produces a momentarily high impulse under his feet and the board's mast joint). In other cases we have catapult like plunges due to strong gusts pulling the rig and sometimes also the rider, who is fixed to the rig with the harness, forward onto the nose part of the board. This can lead to hits with the front of the boom or body parts of the rider into the surface of the nose part of the board. There are also some spectacular moves (e.g. the so called “Willy Skipper”) requiring that the rider lands feet first on the nose this way producing relatively high impact forces. The second class of main failure mechanism are bending loads coming from overturning of so called loop jumps, landing between waves or so called nose or tail dives after high jumps.
Within those two classes of failure mechanisms we here concentrate on the following critical situations:

1. impact load on the board’s nose surface due to hard contact with either body parts of the rider or the rig (see fig. 4)
2. impact load in the foot pad area (under the foot straps) due to flat landing
3. bending load due to landing on or between two waves, where nose and tail are supported by the peaks of the waves while the rest of the board hangs unsupported over the trough
4. bending load caused by hard tail first landing
5. skag hits reef
6. bending load caused by hard nose dive landing or due to over rotation after loop jumps

During our investigation we had to realise that in almost all cases of board destruction it was rather impossible to reconstruct the force and momentum situation in the moment of failure in detail. This was mainly due to the fact that the riders could only give vague information about

their speed, height of the jump (fig. 3), buffer effect of the sail during lading, momentum of rotation etc. or in some cases even their own weight. Further, the investigated boards, though in principle of similar shape and structure, differed widely in details concerning the number of used laminate reinforcements, thicknesses of distinct parts of the boards, used materials within the layered structure and their order (glass fibre, carbon fibre, honeycomb reinforcements…) etc.. Under these circumstances it doesn't seem reasonable to assume concrete load conditions and board constructions. One rather should apply typical load distributions simulating the critical situations and see whether or not the resulting stress distributions coincide with the observed board failure. Thus, we have constructed a relatively simple "model windsurfing board" out of either a layered half space or a layered thick plate model in accordance with the load problem in question. In order to describe board reinforcements in lateral direction, a stability weight function has been introduced in some cases. This weight function is directly related to the lateral change of thickness of the laminate structure.

The first two problems 1 and 2 can be tackled by applying the half space model. We use the material parameters given in table 1 and 2. The water was assumed as to act as some kind of substrate supporting the board structure during the impact such that it could be modelled as being elastic. Here it was of absolutely no importance which concrete elastic parameters for the "substrate" were chosen. As a series of trial evaluations showed the "water-parameters" could be anywhere between rigid and extremely soft without significantly changing the stress distribution within the surface part of the board we are interested in here. Further, as explained above we are just interested in the resulting stress distribution and not any absolute values. Thus, the coefficients of the Young's modulus tensor are given as a function of a parameter E, where a concrete number can be assigned to as soon as concrete board structures are chosen and absolute forces are known. For the resulting qualitative stress distribution however, only the geometrical conditions and the relative material properties of the layers are of importance. Because we are using the half space and the thick plate model we have to treat the results in the vicinity of the boards edges with great caution. But it had been shown experimentally and theoretically [39] that even in the case of a sharp rectangular edge (quarter space) the elastic field near the contact does not differ more than about 15 % from the half space model as long as the distance from the edge does not fall below one contact radius. But as we here only have blunt "edges" and all contacts and failures considered are placed respectively found close to the board's middle, the maximum error might be about 10%, which will suffice for our qualitative failure discussion.

At first we investigate the effect of the impact load on the foam core of the board (fig. 5):

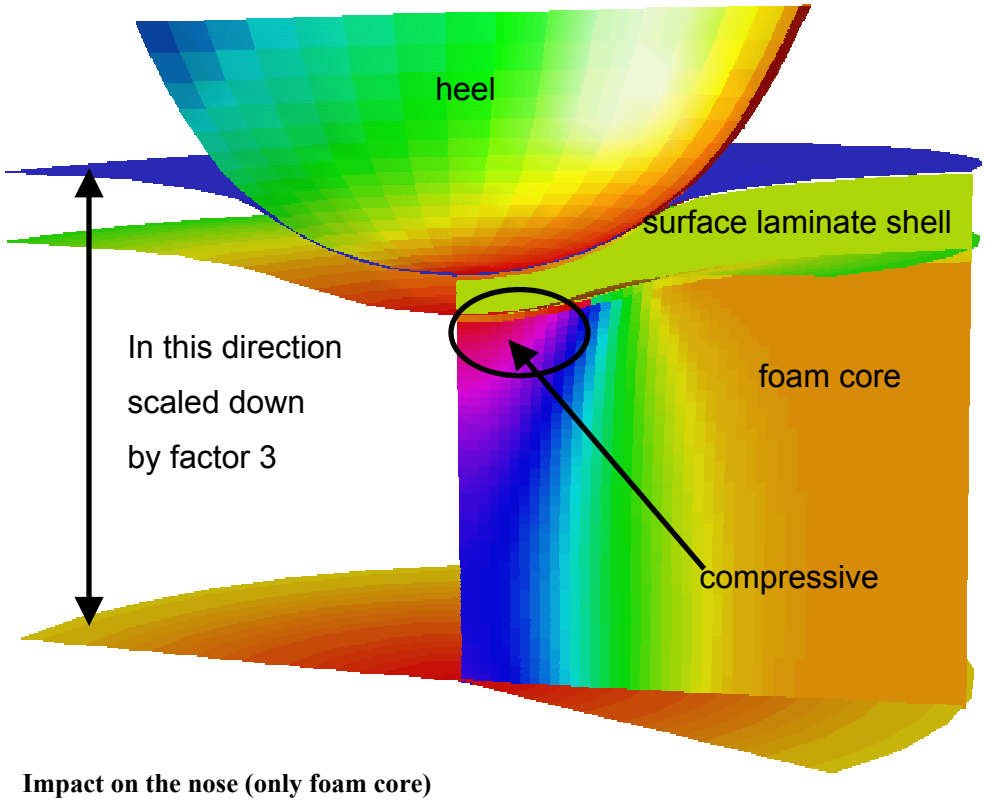


**Fig. 5 Impact on the nose (only foam core)**

As we know from investigating damaged boards, the foam is compressed under the contact zone. It often delaminates from the laminate surface shell (monochrome drawn layer in fig. 5) thus, building a vacancy and leaving the laminate shell unsupported. The figure shows the hydrostatic stress having a strong compressive maximum directly under the indenter (e.g. heel of the rider or front part of the boom…) leading to the material compression. In figure 6 the radial stress within the laminate shell is presented.

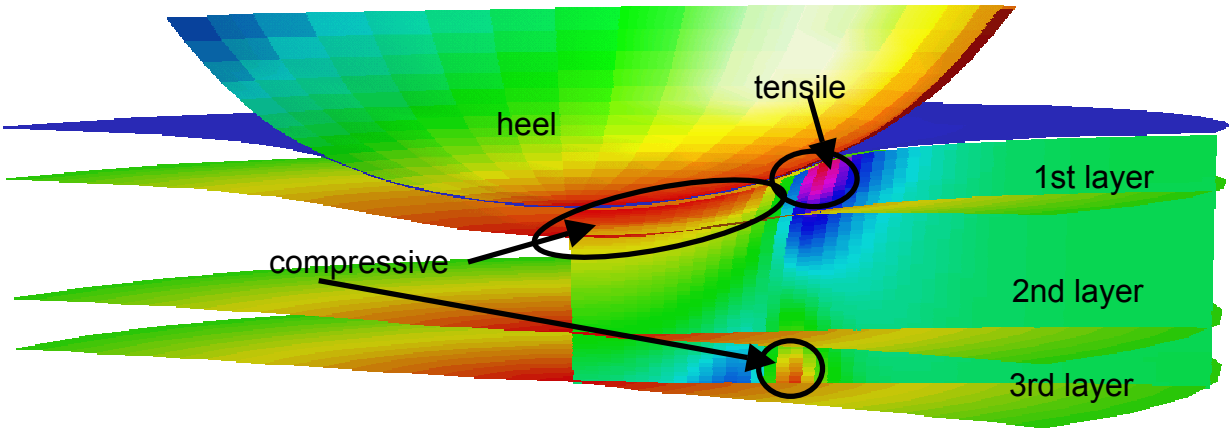


**Fig. 6 Impact on the nose (only laminate shell)**

It shows a pronounced tensile stress maximum at the contact rim which might lead to mode I fracture (Hertzian cone crack). And in fact this type of failure could be observed rather often on the front surface part of windsurfing boards (figure 7: due to its anisotropy the Hertzian here runs along main fibre direction of the laminate tissue structure).

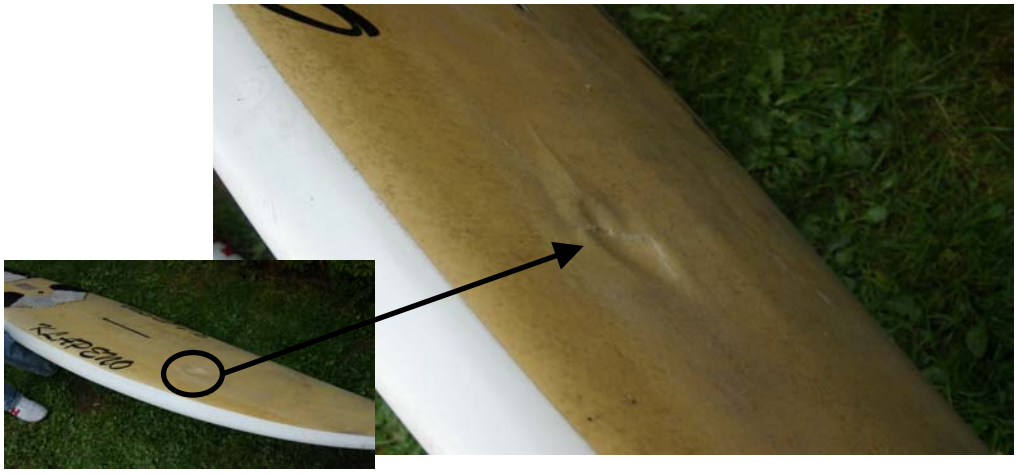

**Fig. 7 Surface fracture damage due to impact load**

Under extreme conditions (Fig. 8: Damaged nose part of a windsurfing board after huge impact: the rider (about 75kg) fell foot first from a height of about 3 meters directly onto the nose of his board) the impact might be even so strong that the board breaks through completely.

**Fig. 8 Complete nose damage due to impact load**

The picture changes completely when the impact load is applied onto the foot pad area (problem 2). Here elongated or star like cracks coming from the contact centre are observed rather than circular cracks (see small photograph in figure 10). This becomes clear when we investigate the radial stresses within the laminate under the rider's heel (fig. 9):

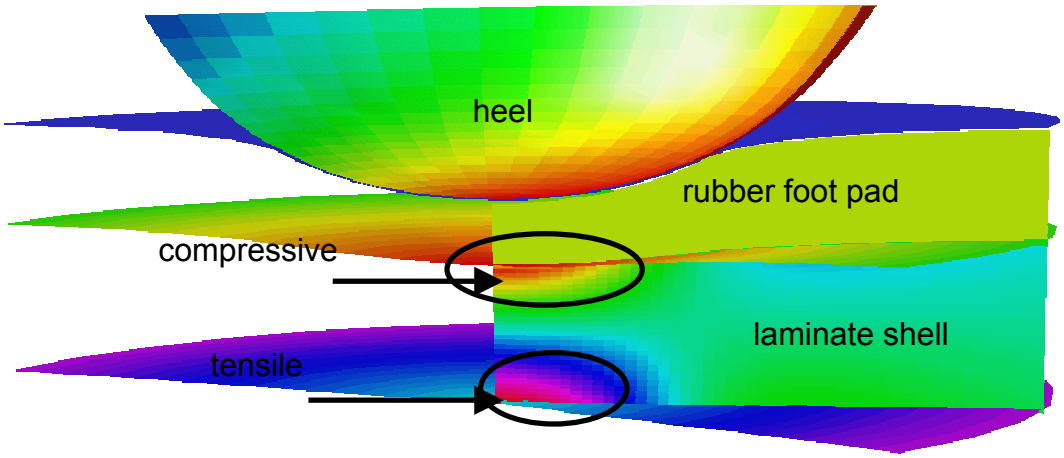


**Fig. 9 Impact on the front foot pad (only laminate shell)**

While, due to the buffer effect of the rubber food pad, there are rather no tensile stresses at the surface of the laminate layer we see, that this time the tensile stress maximum is to be found at the contact centre on the bottom of the laminate shell. But as already seen in problem 1 for the nose part of the board, the foam core is also compressed under the foot pad area due to a maximum of compressive hydrostatic stresses (fig. 10). This effect is widely known by windsurfers, so that second hand boards are always tested here by simply pressing the thumb hard on the area where usually the heel would be in order to see whether impact damage had already occurred.

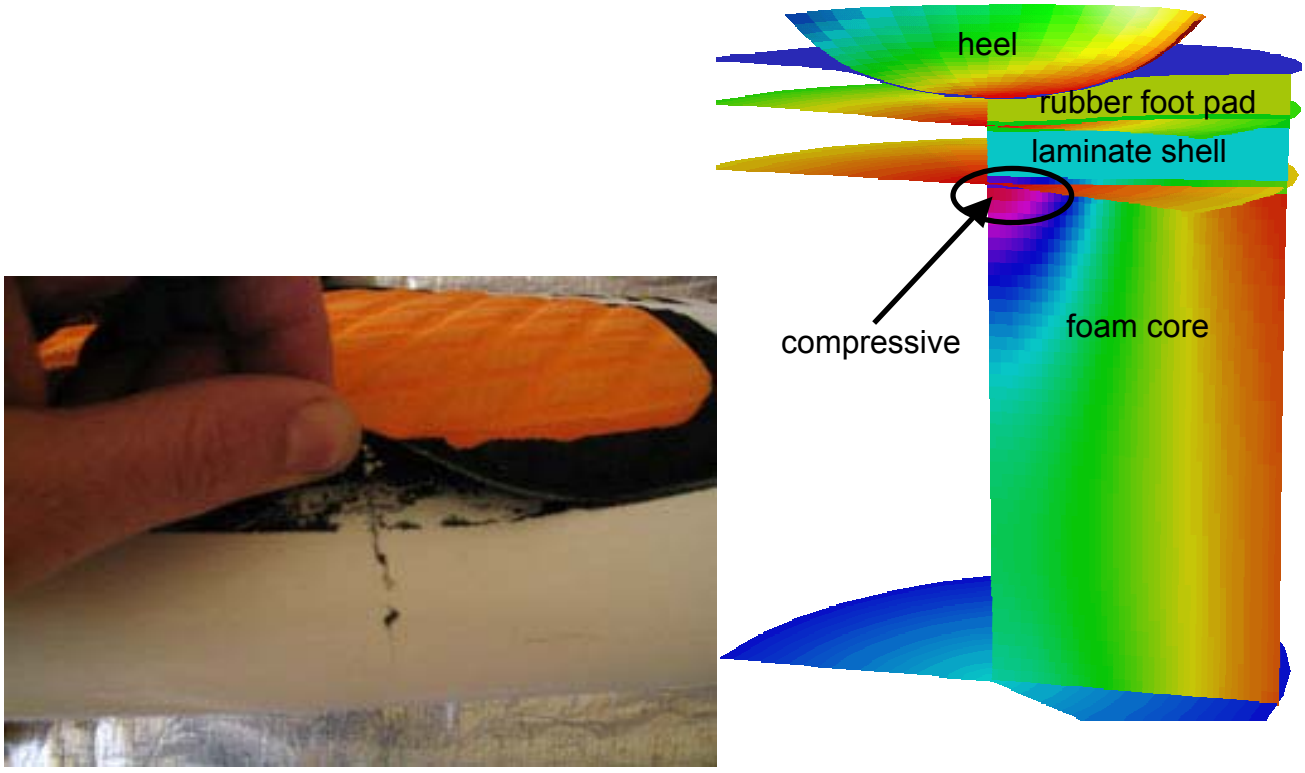


**Fig. 10 Impact on the front foot pad (only foam core)**

The third problem is demonstrated in figure 11 (lower picture):

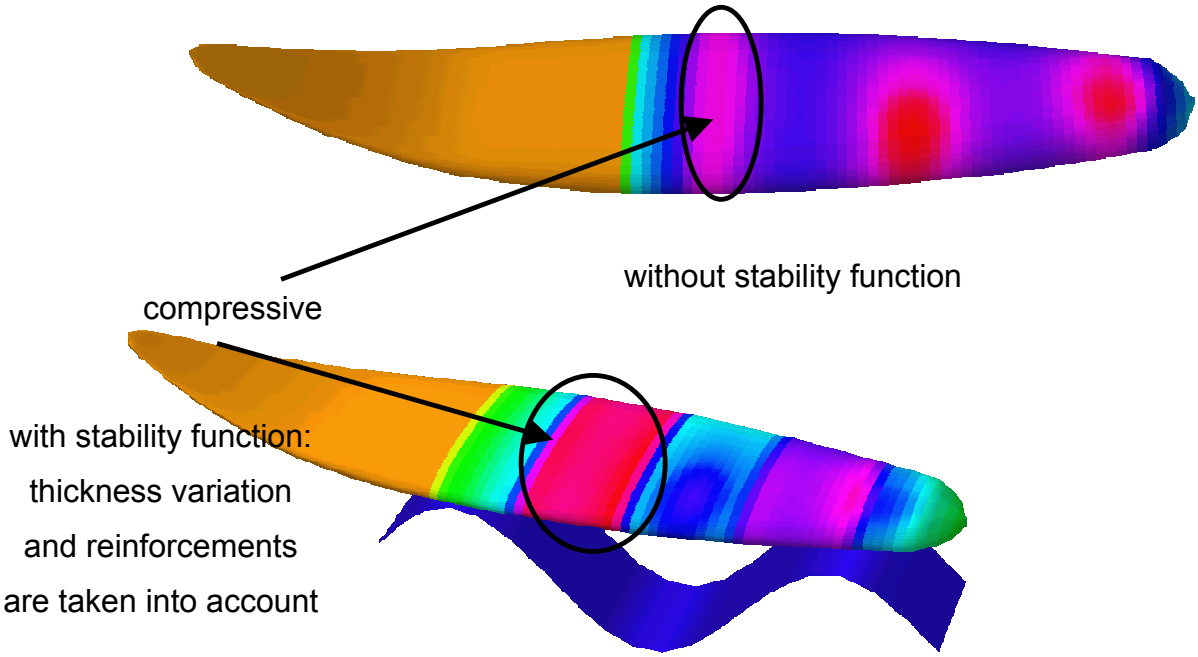


**Fig. 11 (Bad) landing on two ill adjusted waves**

The material parameters used for the evaluation are given in table 3. Analysing the typical load distribution between front and hind leg by using ten different professional windsurfers

put on a so called windsurf simulator equipped with three scales (one for each foot and an additional one for the mast) we obtained a sufficiently consistent load picture. Applying the "model of the thick layered plate" we evaluated the normal stress distribution shown in figure 11 (upper picture). Taking into account that the laminate thickness is not homogenous over the whole surface by introducing a simple "stability function" a refined stress distribution can be obtained (fig. 11, lower picture). Here the stresses shown in figure 11 (upper picture) where simply multiplied with the inverse of the laminate shell thickness. The result, namely a maximum of compressive stresses between mast and front foot pads, is in good agreement with the observed failure (fig. 12).

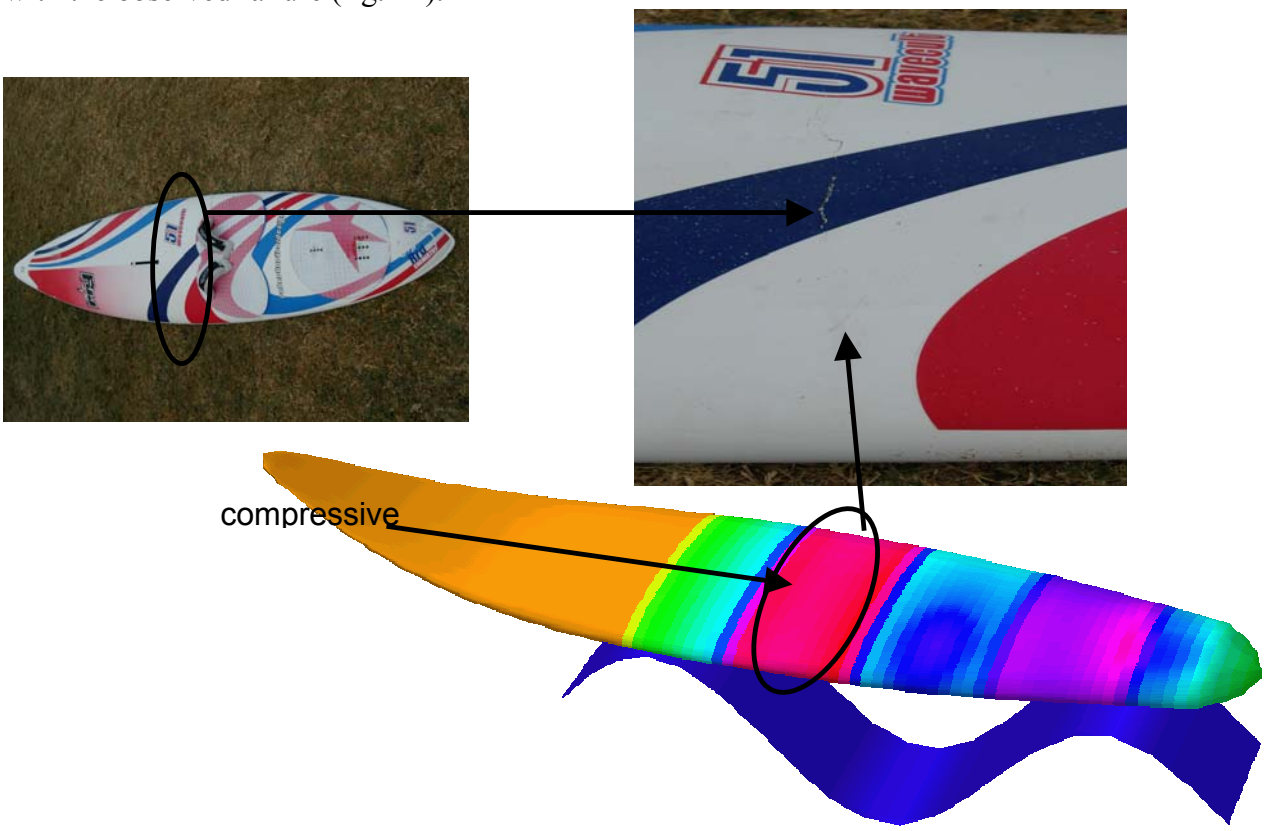


**Fig. 12 Damage due to landing on two ill adjusted waves**

In the case of a hard tail landing (problem 4, demonstrated in the figures 13 and 14) the damage (fracture between the front and hind foot straps as shown in the small photograph of figure 14) is caused by high tensile stresses within the board's surface (see arrow and red area in fig. 14).

**Fig. 13 Tail landing**

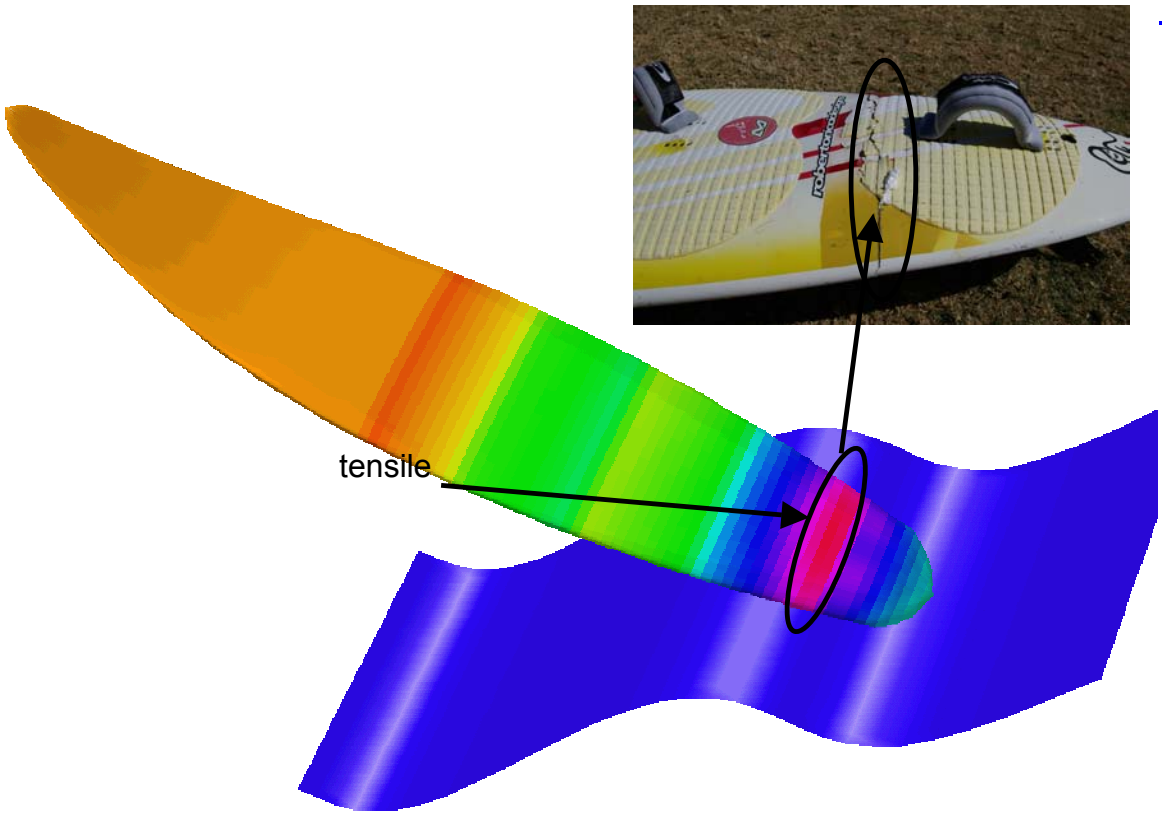


**Fig. 14 Stresses and damage due to hard tail landing**

Similar damage can be observed in the case 5, where the rider hits an under water obstacle (e.g. protruding parts of the reef) with the skag of his windsurfing board. Depending on the speed of the windsurfer, the impact momentum can be big enough to produce huge tensile stresses in the surface laminate (figure 15) right in front of the hind foot strap immediately leading to rapture between the two foot pads (small photograph in figure 15):

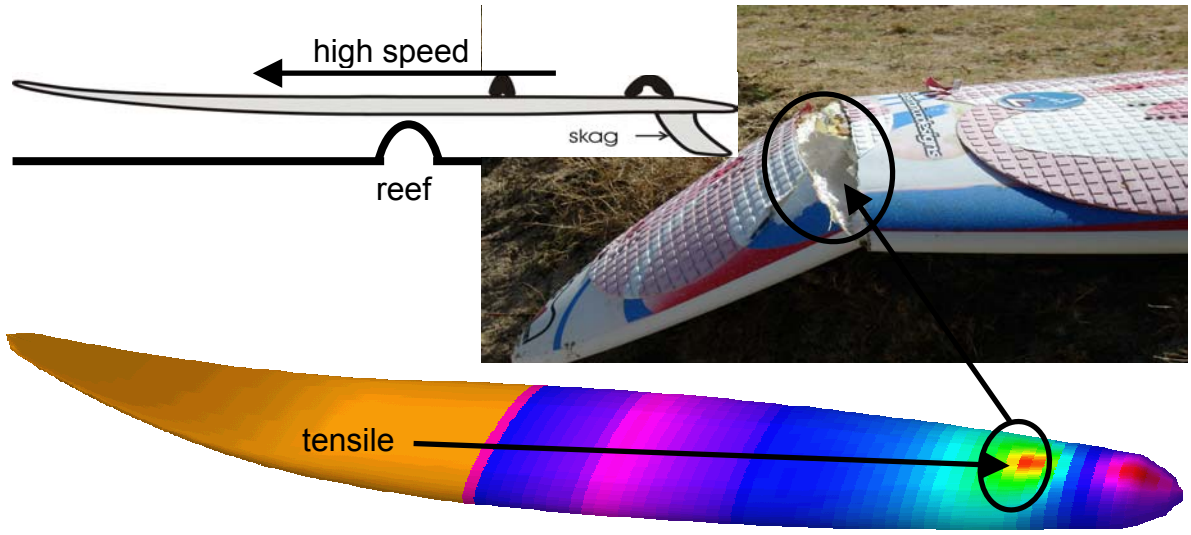


**Fig. 15 Skag hits reef damage**

As one can see the result of this type of impact loading can be quite disastrous. However in the special case of the photograph in figure 15 the “skag hits reef”-impact only initialised the fracture. The rest was done when the rider tried to come back to the shore, planning over a fairly choppy (which means rough) surfing spot, thereby successively bending the board’s tail up and down and so gradually opening the crack more and more until it got almost severed from the rest of the board.

Finally we consider the nose dive landing after an ordinary jump or an overturned front or back loop (problem 6, see figure 16).

**Fig. 16 Example for loop jump**

It can result in high compressive stresses on the surface (figure 17) and tensile stresses on the board's bottom (figure 18) around the mast joint. Here fracture before or behind the mast can occur (figure 19: Here, too, the rider – one of the authors, this time – lost parts of the bottom laminate on the way back to the beach through a very rough shore break zone with relatively high waves.).

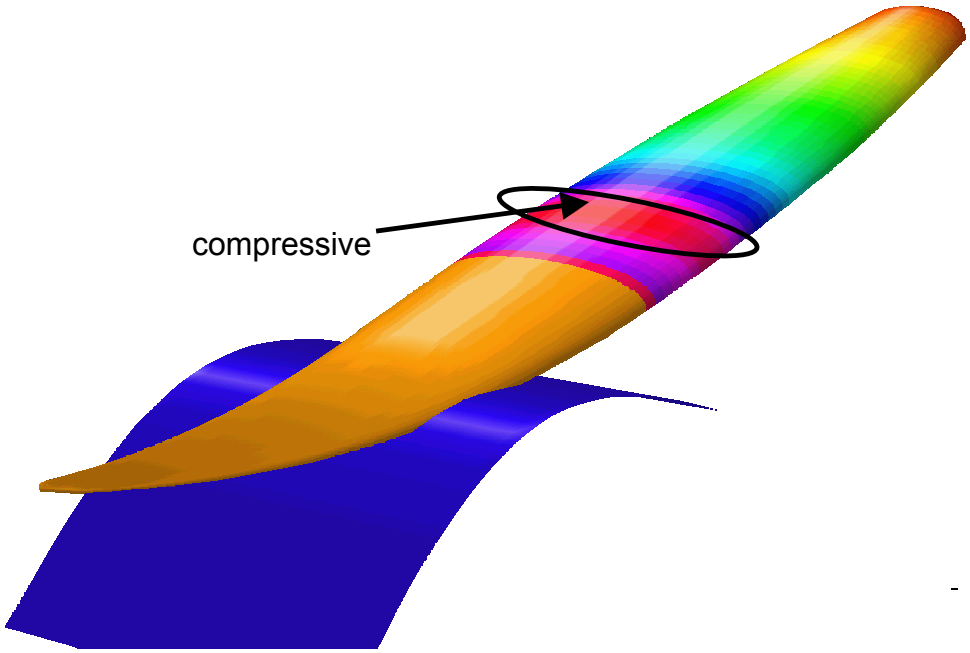


**Fig. 17 Stresses due to hard nose dive (surface)**

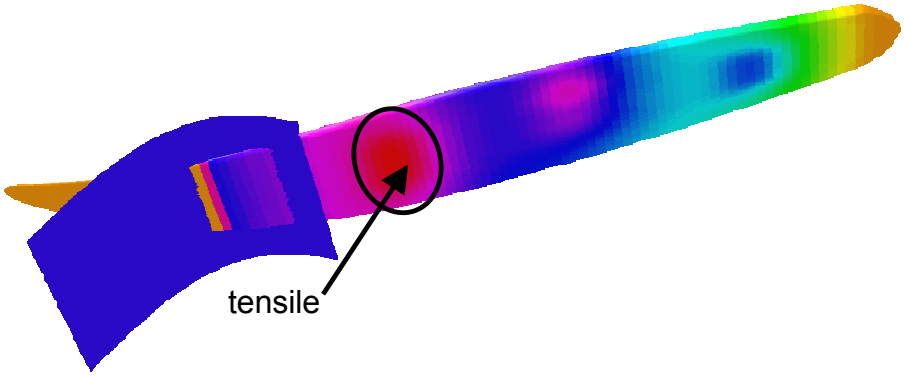


**Fig. 18 Stresses due to hard nose dive (bottom)**

**Fig. 19 Complete bottom fracture due to hard nose dive**

## *Conclusions*

It had been shown, that the typical damage of quite a variety of failure mechanisms occurring on the laminate structures of windsurfing boards can qualitatively described using the layered half space and the layered thick plate model. Laminate thickness variations and reinforcements had been included via a so called stability function. Very good agreement between the observed failures and the location and type of the stress maxima evaluated from the theoretical model was obtained for all considered damages. It was found, that apart from accidents like hitting the reef with the skag or falling on the board's nose, mainly jumps are responsible for most of the observed board failures. Thus, the model might be used as a tool to find out weak spots within the structure of a windsurfing board during shape design and development. The method could also be applied to other laminate structures such as those used in the boat and aircraft or even car industry in order to support the design and construction of impact resistant structures.

## *Acknowledgements*

The authors are thankful to Rocky Legoy from the RRD-Windsurfing centre on Mauritius, Kevin Berichon from Holly Mackerel Productions, Australia, Stefan Gabler and Holger Schneider, Germany for a variety of helpful discussions and demonstrations. We also want to

thank all those riders who damaged their boards, allowed us to interview them in the moment of grieve and even granted us to photograph and thoroughly analyse the board failure.

## *References*

[1] B. Okutan, Composites Part B: Engineering, Vol. 33, No 8, Dec. 2002, 567-578

[2] J. Lopez-Puente, R Zaera, C. Navarro, Composites Part B: Engineering, Vol. 33, No 8, Dec. 2002, 559-566

[3] T. A. Anderson, Composites Part B: Engineering, Vol. 36 (2005), 135-142

[4] T. Gomez-del Rio, E. Barbero, C. Navarro, Composites Part B: Engineering, Vol. 36 (2005), 41-50

[5] N.K. Naik, R. Ramasimha, H. Arya, S.V. Prabhu, N. ShamaRao, Composites Part B: Engineering, Vol. 32 (2001), 565-574

[6] M. De Freitas, A. Silva, L. Reis, Composites Part B: Engineering, Vol. 31 (2000), 199-207

[7] Y. Miyano, M. Nakada, N. Semine, Composites Part B: Engineering, Vol. 35 (2004), 497-502

[8] S. K. Khanna, P. Ranganathan, S.B. Yedla, R.M. Winter, K. Paruchuri, J. Eng. Mat. Technol.125 (2003) 90-96

[9] G. Caprino, A. Langella, V. Lopresto, Composites Part B: Engineering, Vol. 34 (2003), 319-325

[10] I.M. Daniel, E.E. Gdoutos, K.-A. Wang, J.L. Abot, Int. J. Damage Mech., 11 (2002) 309-334

[11] M. Zako, Y. Uetsuji, Int. J. Damage Mech., 11 (2002) 187-202

[12] D. Luo, S. Takezono, K. Tao, H. Minamoto, Int. J. Damage Mech., 12 (2003) 141-162

[13] H. Altenbach, Z. angew. Math. Phy. 51 (2000) 629-649

[14] R. Akkerman, Composites Part B: Engineering, Vol. 33 (2002), 133-140

[15] H.-L. Yeh, H.-Y. Yeh, Composites Part B: Engineering, Vol. 31 (2000), 57-64

[16] P. Thamburaj, M. H. Santare, J. Eng. Mat. Technol.125 (2003) 412-417

[17] B. Shan, A. A. Pelegri, J. Eng. Mat. Technol.125 (2003) 353-360

[18] J.W. Park, Y.H. Kim, Computational Mechanics, Vol. 29, No. 3, 226-242

[19] V. M. Harik, J. Eng. Mat. Technol.125 (2003) 385-393

[20] N. Pai, A. Kaw, M. Weng, Composites Part B: Engineering, Vol. 34 (2003), 405-413

[21] C.C. Chao, C.Y. Tu, Composites Part B: Engineering, Vol. 30 (1999), 9-22

[22] C.Y. Tu, C.C. Chao, Composites Part B: Engineering, Vol. 30 (1999), 23-41

[23] N. Schwarzer, L. Geidel, FunnyIndenter: free software demonstration package for the evaluation of the elastic field of arbitrary combinations of normal and tangential loads of the type "load~ $\sum_{n=1}^{6} c_n * r^n \sqrt{a^2 - r^2}$ " (with n=0,2,4,6), available from the internet at: http://www.esae.de (contact: p.heuer@esae.de)

[24] N. Schwarzer, Arbitrary load distribution on a layered half space, ASME Journal of Tribology, 122 (2000) 672 – 681

[25] H. Gao, C.-H. Chiu, J. Lee, Elastic contact versus indentation modelling of multi-layered materials, Int. J. Solids Structures 29 (1992) 2471-2492

[26] C. Saizonou, R. Kouitat-Njiwa, J. von Stebut, Surface engineering with functionally graded coatings: a numerical study based on the boundary element method, Surf. Coat. Technol. 153 (2002) 290-297

[27] A. E. Giannakopoulos, P. Pallot, J. Mech. Phys. Solids 48 (2000) 1597

[28] A. E. Giannakopoulos, Thin Solid Films 332 (1998) 172

[29] A. E. Giannakopoulos, S. Suresh, Int. J. Solids Structures 34 (1997) 2393

[30] S. M. Aizikovich, V. M. Alexandrov, J .J. Kalker, L. I. Krenev, I. S. Trubchik, Int. J. Solids Structures 39 (2002) 2745

[31] D. S. Stone, J. Mater. Res. 13 (1998) 3207

[32] V. Linss, N. Schwarzer, T. Chudoba, M. Karniychuk, F. Richter: "Mechanical Properties of a Graded BCN Sputtered Coating with VaryingYoung's Modulus: Deposition, Theoretical Modelling and Nanoindentation", Surf. Coat. Technol., in Press, Corrected Proofs, doi:10.1016/j.surfcoat.2004.06.010

[33] T. Chudoba, N. Schwarzer, V. Linss, F. Richter: „Determination of Mechanical Properties of Graded Coatings using Nanoindentation", proceedings of the ICMCTF 2004 in San Diego, California, USA, also in Thin Solid Films (2004): 469-470C pp. 239-247

[34] A. I. Lurje: „Three Dimensional Problems of the Theory of Elasticity", Interscience Publishers, 1964

[35] N. Schwarzer: „Modelling of the mechanics of thin films using analytical linear elastic approaches", Habilitationsschrift der TU-Chemnitz 2004, FB Physik Fester Körper, http://archiv.tu-chemnitz.de/pub/2004/0077

[36] A. J. Jerri: "Integral and discrete transforms with applications and error analysis", Marcel Dekker, Inc., New York, 1992

[37] V. I. Fabrikant: "Application of potential theory in mechanics: A Selection of New Results", Kluver Academic Publishers, The Netherlands, 1989

[38] ELASTICA, software for the calculation of stresses and deformations in coated systems, ESAE, Germany, free trial version available in the internet at: http://www.esae.de.

[39] N. Schwarzer, I. Hermann, T. Chudoba, F. Richter: ”Contact Modelling in the Vicinity of an Edge”, Surface and Coatings Technology 146-147 (2001) 371-377

## *Tables*

Table 1: Material Parameters for the board’s nose part

| **Layer** | **$A_{11}$** | **$A_{12}$** | **$A_{13}$** | **$A_{33}$** | **$A_{44}$** | **Thickness** |
|---|---|---|---|---|---|---|
| **Transversaly isotropic** | $75*E_1$ | $15*E_1$ | $1.2*E_1$ | $1.8*E_1$ | $1.6*E_1$ | 0.5mm |
| **Isotropic** | $1.2*E_2$ | $0.4*E_2$ | $0.4*E_2$ | $1.2*E_2$ | $0.4*E_2$ | 2mm |
| **Transversaly isotropic** | $75*E_1$ | $15*E_1$ | $1.2*E_1$ | $1.8*E_1$ | $1.6*E_1$ | 0.5mm |
| **Foam core Isotropic** | $1.2*E_3$ | $0.4*E_3$ | $0.4*E_3$ | $1.2*E_3$ | $0.4*E_3$ | 82mm |
| **Transversaly isotropic** | $75*E_1$ | $15*E_1$ | $1.2*E_1$ | $1.8*E_1$ | $1.6*E_1$ | 0.5mm |
| **Isotropic** | $1.2*E_2$ | $0.4*E_2$ | $0.4*E_2$ | $1.2*E_2$ | $0.4*E_2$ | 4mm |
| **Transversaly isotropic** | $75*E_1$ | $15*E_1$ | $1.2*E_1$ | $1.8*E_1$ | $1.6*E_1$ | 0.5mm |

$E_2$=6 $E_1$=100 $E_3$=E

Table 2: Material Parameters for the board’s foot pad area

| **Layer** | **$A_{11}$** | **$A_{12}$** | **$A_{13}$** | **$A_{33}$** | **$A_{44}$** | **Thickness** |
|---|---|---|---|---|---|---|
| **Rubber pad Isotropic** | $1.2*E_0$ | $0.4*E_0$ | $0.4*E_0$ | $1.2*E_0$ | $0.4*E_0$ | 6mm |
| **Transversaly isotropic** | $75*E_1$ | $15*E_1$ | $1.2*E_1$ | $1.8*E_1$ | $1.6*E_1$ | 0.5mm |
| **Isotropic** | $1.2*E_2$ | $0.4*E_2$ | $0.4*E_2$ | $1.2*E_2$ | $0.4*E_2$ | 3mm |
| **Transversaly isotropic** | $75*E_1$ | $15*E_1$ | $1.2*E_1$ | $1.8*E_1$ | $1.6*E_1$ | 0.5mm |
| **Transversaly isotropic** | $75*E_1$ | $15*E_1$ | $1.2*E_1$ | $1.8*E_1$ | $1.6*E_1$ | 0.5mm |
| **Isotropic** | $1.2*E_2$ | $0.4*E_2$ | $0.4*E_2$ | $1.2*E_2$ | $0.4*E_2$ | 4mm |
| **Transversaly** | $75*E_1$ | $15*E_1$ | $1.2*E_1$ | $1.8*E_1$ | $1.6*E_1$ | 0.5mm |

| | | | | | | |
|---|---|---|---|---|---|---|
| **isotropic** | | | | | | |
| **Foam core Isotropic** | 1.2*$E_3$ | 0.4*$E_3$ | 0.4*$E_3$ | 1.2*$E_3$ | 0.4*$E_3$ | 70mm |
| **Transversaly isotropic** | 75*$E_1$ | 15*$E_1$ | 1.2*$E_1$ | 1.8*$E_1$ | 1.6*$E_1$ | 0.5mm |
| **Isotropic** | 1.2*$E_2$ | 0.4*$E_2$ | 0.4*$E_2$ | 1.2*$E_2$ | 0.4*$E_2$ | 4mm |
| **Transversaly isotropic** | 75*$E_1$ | 15*$E_1$ | 1.2*$E_1$ | 1.8*$E_1$ | 1.6*$E_1$ | 0.5mm |

$E_2$=10 $E_0$=6 $E_1$=100 $E_3$=E

Table 3: Material Parameters used for the bending load calculations

| **Layer** | **$A_{11}$** | **$A_{12}$** | **$A_{13}$** | **$A_{33}$** | **$A_{44}$** | **Thickness** |
|---|---|---|---|---|---|---|
| **Transversaly isotropic** | 75*$E_1$ | 15*$E_1$ | 1.2*$E_1$ | 1.8*$E_1$ | 1.6*$E_1$ | 0.5mm |
| **Isotropic** | 1.2*$E_2$ | 0.4*$E_2$ | 0.4*$E_2$ | 1.2*$E_2$ | 0.4*$E_2$ | 4mm |
| **Transversaly isotropic** | 75*$E_1$ | 15*$E_1$ | 1.2*$E_1$ | 1.8*$E_1$ | 1.6*$E_1$ | 0.5mm |
| **Foam core Isotropic** | 1.2*$E_3$ | 0.4*$E_3$ | 0.4*$E_3$ | 1.2*$E_3$ | 0.4*$E_3$ | 80mm |
| **Transversaly isotropic** | 75*$E_1$ | 15*$E_1$ | 1.2*$E_1$ | 1.8*$E_1$ | 1.6*$E_1$ | 0.5mm |
| **Isotropic** | 1.2*$E_2$ | 0.4*$E_2$ | 0.4*$E_2$ | 1.2*$E_2$ | 0.4*$E_2$ | 4mm |
| **Transversaly isotropic** | 75*$E_1$ | 15*$E_1$ | 1.2*$E_1$ | 1.8*$E_1$ | 1.6*$E_1$ | 0.5mm |

$E_2$=6 $E_1$=100 $E_3$=E